9th INTERNATIONAL SYMPOSIUM ON MEASUREMENT AND QUALITY CONTROL (9th ISMQC)
November 21 – 24, 2007, IIT Madras

OPTICAL MEASURING TECHNOLOGIES AND LASER SYSTEMS FOR INDUSTRIAL APPLICATIONS

Chugui, Yu. V.

(Finogenov, L. V., Plotnikov, S. V., Potashnikov, A. K. and Verkhogliad, A. G.)
Technological Design Institute of Scientific Instrument Engineering (TDI SIE)
Siberian Branch of the Russian Academy of Sciences (SB RAS)
41, Russkaya str., Novosibirsk, 630058, Russia
Tel.: +7 (383) 333-27-60 Fax: +7 (383) 332-93-42 E-mail: chugui@tdisie.nsc.ru

Abstract: *Modern industry takes novel optical measuring systems with micron resolution and productivity up to 10^5 meas/s, as well as laser technologies for solving actual tasks, including safety problems for mining, atomic and railway industries. New measurement approaches, including 3D diffraction, Fresnel diffraction method, 3D hole inspection are presented. We have researched, developed and tested some novel optical measuring systems and laser technologies. Experimental results and performances of the optical measuring and laser systems are given.*
Key words: *optical measuring technology, laser technology, 3D inspection.*

1. INTRODUCTION

Solving many actual safety problems in mining, oil, atomic and railway industries as well as in science takes noncontact optical measurement technologies with micron resolution and productivity from 500 to 10^5 meas/s (Brown et al., 1992). We have investigated new measurement approaches, including 3D diffraction, Fresnel diffraction method, 3D hole inspection, as well as developed, implemented and tested some novel optical measuring systems and laser technologies.

Constructive method for calculations of Fraunhofer patterns of the 3D objects with clear shadow projections is presented. Dependencies between the characteristic parameters of the diffraction patterns and the geometric dimensions of 3D typical objects are given.

Modern industry and market impose stringent requirements upon the precision, price, mass, and size of the noncontact meters for dimensional inspection. One of the available possibilities is to use Fresnel diffraction patterns. We have presented here some results on Fresnel measuring method.

As it is known, numerous articles with holes are produced in industry. We have developed optical inspection method on the basis of diffraction optical element (DOE), as a ring diffractive focuser. It allows us to create a small-size probe to inspect the hole diameter, nonstraightness of hole axis, deviation of the surface shape from a cylindrical one, and the surface quality.

Laser material processing (cutting, welding) of 3D large-size objects and treatment (ablation) of their surfaces take multifunctional universal laser technological system. Such system (LSP-2000) was developed at TDI SIE. It has 5-coordinate table with CNC system with displacement range of $3 \times 3 \times 0{,}6$ m^3 (position error less than 10 μm) and changeable Nd-YAG lasers for material processing and treatment. Below the LSP-2000 technical peculiarities and performances are given.

Effective investigation of non-linear processes in block structures of geo medium requires comprehensive measurement of wave, deformation and power parameters using the multi-channel measuring systems. For measurement the rocks stress and prevention the mountain impact we have developed a set of optical-electronic deformers and systems for modeling and investigation of nonlinear deformation wave processes.
Safety of nuclear reactors and ensuring their high exploitation reliability take 100 % noncontact inspection of fuel assemblies, fuel elements, grid spacers and also fuel element surface inspection with micron resolution. We have developed and produced at TDI SIE some measuring technologies for Russian atomic plants.

For increasing the safety of railways we have developed high-speed laser noncontact method and produced automatic laser diagnostic system COMPLEX for noncontact inspection of geometric parameters of wheel pairs for running trains. Principle of self-scanning for running freight cars and testing results for system COMPLEX are given.

2. 3D DIFFRACTION

For the 3D bodies with clear shadow projection, which represent a wide class of objects, the shadow model appears to be approximate and may lead to considerable errors. Since the existing strict and approximate solutions for diffraction problem are extremely difficult for engineering applications, we have suggested and developed the constructive theory for diffraction patterns and image formation, as well as for filtering of 3D objects with constant thickness. Such theory is simple enough, physically obvious and at the same time sufficiently strict for practical applications.

2.1. The constructive method for calculation of diffraction patterns of extended objects

It is based on the model of equivalent diaphragms (distributions) for 3D objects of constant thickness with perfectly absorbing, perfectly reflecting and grey inner surfaces (Fig. 1). According to this model the front and rear faces of the object give the main contribution into the field. The influence of their inner surfaces on the diffraction component is supposed to be negligible small and, therefore, results in the absorption or reflection of the waves diffracted on the front face of the object. As a result, the problem of light diffraction on volumetric bodies is reduced to the analysis of diffraction phenomena on the plane objects (described by binary or bipolar boundary functions), which are located in space. It permits to apply the standard Fourier-optical methods for the calculation in the Kirchhoff-Fresnel approximation.

Fraunhofer diffraction patterns of such typical elements of extended bodies as volumetric edge and 3D slit with the absorbing and reflecting inner faces have been under investigation. In case of the 3D *perfectly absorbing asymmetric edge* with extension (thickness) *d* (Fig. 1(a)), according to the model of the equivalent diaphragms (Fig. 1, b), the boundary functions are the following: f(x) = Y(x), g(x_1) =Y(x_1 - C), and the spectrum is described by equation:

$$F_1(\theta) = \pi\delta(\kappa\theta) + \frac{\widetilde{Y}(d\theta - C)}{jk\theta} + \widetilde{Y}(C)\frac{e^{-jk\theta C}}{jk\theta}\exp\left(\frac{jkd\theta^2}{2}\right), \quad (1)$$

where δ(z) is the Dirack delta-function, $\widetilde{Y}(z) = e^{j\pi/4}(\lambda d)^{-\frac{1}{2}}\int_{-\infty}^{+\infty} Y(x)\exp\left[\frac{jk(x-z)^2}{2d}\right]dx$ is the Fresnel transform of the Heaviside step function Y(z) ($k = 2\pi/\lambda$ is the wave number, λ is the wavelength).

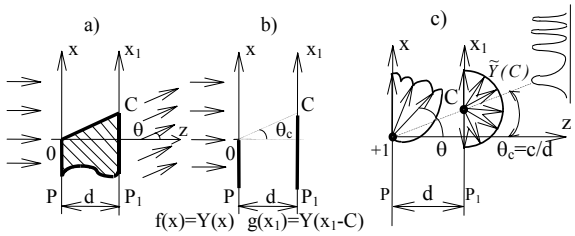

Fig. 1. The 3D *perfectly absorbing asymmetric edge* (a), its equivalent diaphragm model (b), and the generalized two-point source model of diffraction (c).

Model of field formation (accurate to the factor $k\theta$) can be presented in the form of the generalized delta sources with the corresponding amplitude and radiation patterns at the boundary points x = 0 and x = C (Fig. 1(c)).

In case of the light diffraction by the 3D *perfectly absorbing asymmetric slit* front and back holes of which have different widths *D* and D_1 (let $D > D_1$), so that centres of these holes are shifted by *b,* one can obtain the following formula for the spectrum of the 3D slit (Fig. 2(a)):

$$F_2(\theta) = \frac{1}{jk\theta}\left\{e^{jk\theta D/2}\widetilde{\mathrm{Rect}}\left(\frac{d\theta - 0.5D - b}{D_1}\right) - e^{-jk\theta D/2}\widetilde{\mathrm{Rect}}\left(\frac{d\theta + 0.5D - b}{D_1}\right) + e^{jkd\theta^2/2}e^{jk\theta(0.5D_1 - b)}\widetilde{\mathrm{Rect}}\left(\frac{b - 0.5D_1}{D}\right) - e^{jkd\theta^2/2}e^{-jk\theta(0.5D_1 + b)}\widetilde{\mathrm{Rect}}\left(\frac{b + 0.5D_1}{D}\right)\right\}, \quad (2)$$

where $\widetilde{\mathrm{Rect}}(z)$ is the Fresnel image of the rectangular function $\mathrm{rect}(z)$. The generalized point model in the case of diffraction on a 3D slit has four sources with the corresponding radiation patterns (Fig. 2(b)). Their interference determines the distinctive peculiarities being introduced into spectrum by the extension *d* of the object. For example, in case of light diffraction by a symmetric volumetric slit (D=D_1, b=0) the volumetric effects in the low-frequency domain of its spectrum reduce to the addition of spectrum modulation by low-frequency ("Fresnel") oscillations with the minima when $\varphi_m = \sqrt{(2m+1)\lambda/d}$ *(m = 0,1,2..)* and also to the decrease of frequency of high-frequency ("Fraunhofer") oscillations with characteristic size $\theta_1^{(0)} = \lambda/D$ (Fig. 3).

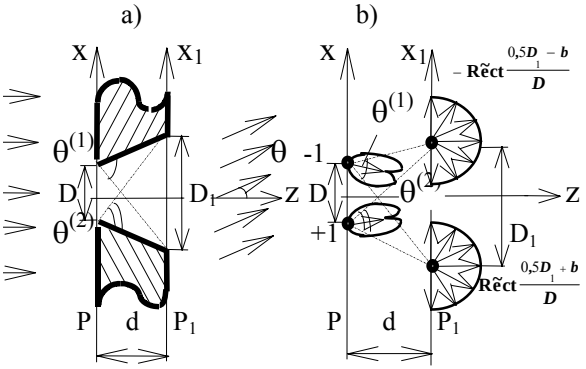

Fig. 2. The 3D perfectly absorbing asymmetric slit (a) and its generalized four-point source model of diffraction (b).

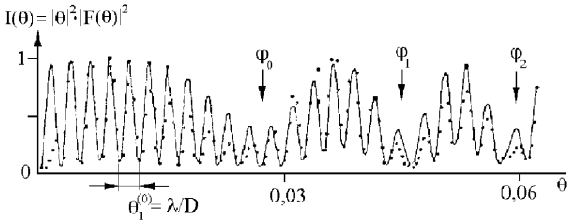

Fig. 3. Experimental results: spectrum of the 3D symmetric perfectly absorbing slit with d=1 mm and D=0.277 mm. Points are experimental data, solid line is calculated spectrum.

Under the spectrum calculating of 3D *perfectly reflecting* objects, one should take into account the reflecting effects of diffracted waves by the inner surfaces of the object. We have investigated in detail the light diffraction on the extended symmetric objects made of metal (Fig. 4 (a)). Due to phase change of the reflected

wave by π, according to the model of the equivalent diaphragms (Fig. 4 (b)), boundary functions for this 3D object are the following: f(x)=sign(x), g(x$_1$)=Y(x$_1$). The spectrum of 3D *perfectly reflecting symmetric edge* is described by the following function:

$$F_3(\theta) = \pi\delta(k\theta) + 2\widetilde{Y}(d\theta)/(jk\theta) \qquad (3)$$

It is essential in this case that the secondary light diffraction on the back face is absent (Fig. 4(c)). Using Eq. (3), it is not difficult to obtain the spectrum of 3D *perfectly reflecting symmetric metallic slit* taking into account the single wave reflection from their inner surfaces:

$$F_3(\theta) = \frac{2}{jk\theta}\left\{\begin{array}{l} e^{jk\theta D/2}\,\widetilde{Re}ct\left(\dfrac{d\theta - 0.5D}{D}\right) \\ -e^{-jk\theta D/2}\,\widetilde{Re}ct\left(\dfrac{d\theta + 0.5D}{D}\right) \end{array}\right\} \qquad (4)$$

2.2. Determination of 3D objects parameters by spectrum

Using the previous results, the dependencies are determined between their characteristic parameters and the geometric dimensions of 3D absolutely absorbing and reflecting edge and slit.

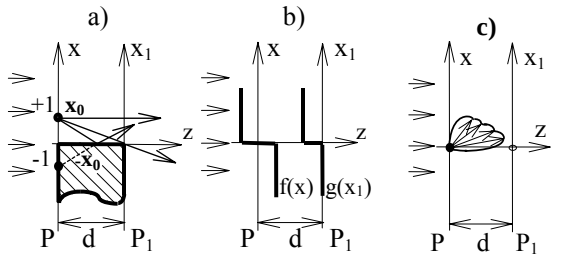

Fig. 4. The 3D *symmetric perfectly reflecting edge* from metal (a), its equivalent field distribution model (b) and the generalized one-point source model (c).

For instance, in the case of the 3D *absolutely absorbing symmetric slit* the minima of its spectrum are quasi-equidistant for $N = \theta_{cr}/\theta_0 >> 1$, where $\theta_{cr} = \sqrt{\lambda / d}$ is the critical angle, under which the 3D effects are significant, θ_0 is the observation angle:

$$\theta_n = n\frac{\lambda}{D}\left(1 + \frac{1}{\sqrt{2\pi N}}\right) \approx \frac{n\lambda}{D - 0.225\sqrt{\lambda d}}, \qquad (5)$$

The extension *d* of the 3D slit leads to an increase of the fringe period. This is equivalent to the action of a plane slit with the efficient width $\widetilde{D} = D - 0.225\sqrt{\lambda d}$.

Since formula (5) does not permit to find simultaneously the dimensions *D* and *d*, the method for their determination is proposed on the basis of the *d* estimation using the angle position of the minima φ_m of the Fresnel modulation in spectrum:

$$d = (2m+1)\,\lambda / \varphi_m^2, \quad D = 0.225\sqrt{\lambda d} + n\lambda/\theta_n, \qquad (6)$$

According to estimations, the theoretical error of determination the longitudinal dimension with typical parameters of the optical system constitutes ~1%. As for the transverse dimension, the accuracy of its determination (as compared to the traditional method) increases ten times and can constitute ~ 0.1% due to the proposed algorithm.

3. FRESNEL MEASURING METHOD

As for new measuring approach, promising solution is to use Fresnel diffraction method, based on formation and processing of Fresnel image, observed in plane P_2, which is located at distance *z* from the inspected object (Fig. 5).

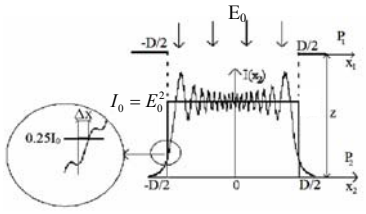

Fig. 5. Fresnel diffraction measurement method: P_1 and P_2 are the object and Fresnel image planes.

Object size *D* is determined by threshold processing of Fresnel image by the I_{thr}=0.25I_0 threshold (I_0 is input intensity) under the condition that Fresnel number $N_{Fr} = D^2/4\lambda z >> 1$. Free space transforming the object image to its Fresnel image with a high accuracy operates as an optical element. It opens up possibilities for the development of compact high performance meters. As this method is studied insufficiently, we have investigated its precision and limiting characterizations (Chugui et al., 2006). The major sources of systematic measurement errors due to non-uniform coherent illumination, edges interference effects are estimated. In case of weak non-uniform illumination $\Delta I << I_0$, correcting algorithm for threshold is the following:

$$\widetilde{I}_{thr}(x_2) = 0.25 I_0(x_2)\cdot[1 + \Delta I/(\sqrt{2\pi}\cdot I_0(x_2))], \qquad (7)$$

where $I_0(x_2)$ is the output intensity at the boundary object points (e.g. for slit object in Fig. 6 $x_2 = \pm 0.5D$). This algorithm allows us to decrease this component error more that 40 times.

We have studied a lower limit D_{low} of measuring

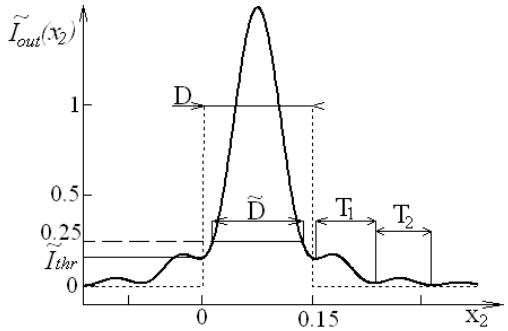

Fig. 6. The inspected slit with size *D*=0.15 mm (dashed) and its Fresnel image (solid) under N=0.43 (z=20 mm)

range for this method. Under $D_{low} \approx \sqrt{\lambda z}$ interference

effect of the diffraction images of object edges is appeared considerably. It leads to a displacement of the threshold level under determination the object boundaries. For example, for this slit the relative error is equal to 18%, using the I_{thr}=0.25I_0 threshold.

We have proposed a new algorithm for Fresnel image processing that ensures significantly the measurement accuracy increase. It takes into account the character of the field in the vicinity of the edge. In this case the threshold $\widetilde{I}_{thr}$ for edge location determination at point x_2=0 at $D\sim\sqrt{\lambda z}$ can be the following:

$$\widetilde{I}_{thr} / I_0 = 0.25 - \frac{1}{2\pi}\sqrt{\frac{\widetilde{T}}{\widetilde{D}}}\cos(\pi\frac{\widetilde{D}}{\widetilde{T}} + \pi/4), \quad (8)$$

where $\widetilde{T} = \sum_{i=1}^{N} T_i / N = \lambda z / \widetilde{D}$ is the average period of modulation and $\widetilde{D}$ is the object size estimation determined by the level $0.25I_0$. Using this algorithm the relative error can be decreased up to 10 times.

4. INSPECTION OF HOLES PARAMETERS USING A RING DIFFRACTIVE FOCUSER

As known, the quality of articles with holes is characterized by the following parameters: straightness, deviation of the diameter from a nominal value and the shape deviation from a cylindrical one, and the quality of the surface. The contact devices for the inspection of holes (plug gauges, like plugs and inside callipers) have significant disadvantages: the rapid wear of the working surfaces, the low efficiency and a high risk of inspected surface damage. The proposed optoelectronic noncontact method using diffractive optical elements (DOE) is free from the above disadvantages.

The method involves formation of ring illumination field (mark) on the inner cylindrical surface of the article under inspection, then detection, and at last processing of the obtained image (Fig. 7). A laser beam impinges to collimator 2 and DOE 3, which forms a ring mark on the inner surface of article 4. The mark is observed with the help of projecting conical mirror 5 and camera 6. The image is processed by computer 7. Device 8 moves the article along optical system axis. With this method, one can inspect the diameter, non-straightness of the hole axis, deviation of the hole shape, and quality of the inner surface.

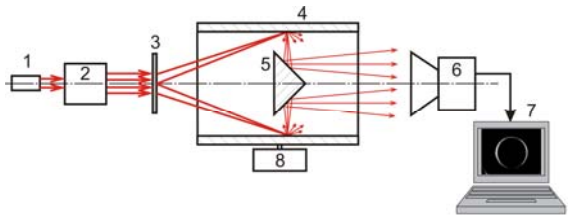

Fig. 7. Principle of holes inspection by DOE: 1 - laser; 2 - collimator; 3 -DOE; 4 - object under inspection; 5 -conical mirror; 6 - CCD-camera; 7 - computer; 8 - device for detail moving.

Measurement of the hole axis non-straightness in different object sections is illustrated in Fig. 8. In position I (a), the axis of the hole coincides with that of the measurement system. The image of the ring mark (b) in the photo detector matrix is a circle with its center at the optical axis. In positions II and III (a), the axis of the article does not coincide with that of the system. Therefore, the images of the ring mark are shifted with respect to the center.

(a) (b)

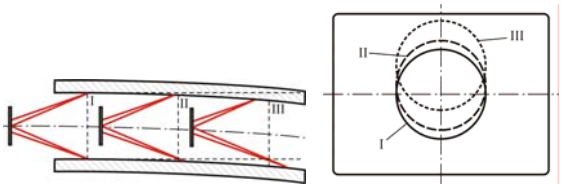

Fig. 8. Modification of the ring mark image versus the hole axis bending; a – object with axis bending; b - ring mark image.

As the diameter of the hole changes, and the optical axis of the system is not shifted with respect to that of the hole, the image of the optical mark is a circle whose radius changes depending on the diameter of the hole. As the diameter of the hole increases, the radius of the circle decreases.

In experiments we have used DOE with the diameter of 40 mm and the minimum period of diffractive zone of 2.5 μm, which was produced by the TDI SIE's circular laser photo plotter CLWS-300/C-M. A standard article with cylindrical step-shaped holes with diameters from 39.3 mm up to 40.7 mm was used. Experimental error didn't exceed of 2.5 μm.

5. LASER TECHNOLOGICAL SYSTEM FOR 3D MATERIAL TREATMENT AND INSPECTION

We have developed laser technological system (LSP-2000) for cutting, welding and surface micro profiling with ablation process, as well as for 3D inspection (Fig. 9). The LSP-2000 system is equipped with two Nd-YAG lasers. The first laser has the following parameters: the pulses repetition frequency is 300 Hz, average power output is 500 Wt, and laser wavelength is 1.064 μm. Its purpose is laser cutting and laser welding of any metals with thicknesses of less then 6 mm. The second laser has pulses repetition frequency of 300 Hz, high pulses power (> 10^7 Wt), laser wavelength is 0.532 μm, average power output is 10 Wt. Its purpose is the ablation of thin metal films on dielectric surfaces. The 5-coordinates (X-Y-Z-φ-θ) robotics for the laser head positioning and CNC control interface is provided for 3D inspection and machining of samples with arbitrary topology. The system spatial working range is about 3 × 3 × 0.6 m^3. Within this range all types of operations can be performed with contour displacement error less than ± 10 μm for any point of trajectory. The LSP-2000 was designed as the precision universal laser inspection and processing system with unique combination of certain parameters / technical characteristics. Uncertainty of this system for coordinate measurements (CMM' regime) is 5

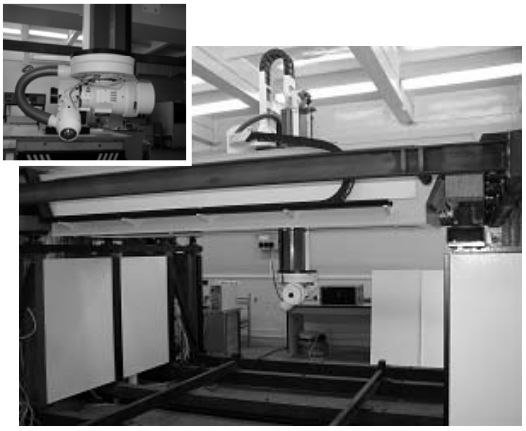

Fig. 9 Laser technological system LSP-2000 and enlarged fragment of its working processing head

μm. This system was developed and produced for Chinese Space Corporation.

6. ROCKS NONLINEAR GEOMECHANICAL STUDY BY MEASURING TECHNIQUES

Investigation of mining-induced movements of structural inhomogeneities of rocks, rock stratum displacement, and deformations takes the measurements of geoblock displacements and strains at different points of a massif. These displacements depend on location of these points relative to underground working contour in geomedia with both natural and induced jointing, and with allowance for structural features (disintegration zones, tectonic faults, pillars or filling masses failed by rock pressure or blasting, etc.). Institute of Mining SB RAS and TDI SIE SB RAS have developed a prototype of a borehole multichannel optical-electronic longitudinal deformometer.

The technical solution of measuring displacements of geoblocks in a rock mass is based on a "slide gauge idea". The idea is realized using a measuring bar, which is fastened inside the massif in a borehole, and a position sensor with its sensing element attached to the rock and capable of moving freely along the bar (Fig. 10).

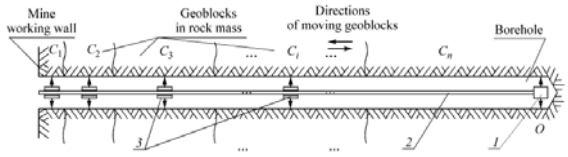

Fig. 10. Scheme of measuring bar and sensors in borehole.

The bar sections and sensors together is a pickup probe. Measuring bar *2* is fastened at the reference point *O* via support *1*. According to the number of measured blocks, sensors *3* are installed on the bar with the sensing elements fastened to the rock at the points C_1, C_2,..., C_n. Having such arrangement, displacement of the *i*-th block under inspection will cause the same displacement of the sensing element of the corresponding sensor along the bar, which is recorded by an electron device.

The developed sensor is based on the position-sensing S3270-type photodetector PSD (Hamamatsu Co). This position sensor equipped by LED has the following characteristics: the measurement range is ± 17.5 mm; the measurement error is ± 0.02 mm. Using these sensors (Fig. 11) we have developed the measuring system providing automatic measurements of longitude shifts and deformations in rocks (actual tests in mine working). For the detailed laboratory testing of models of block geomedia under uniaxial and biaxial loading we have developed a prototype of a micrometer position sensor with a microprocessor data collection system. The error is no more than ± 3 μm and can be reduced to 1 μm.

The information measuring system on the base of electronic micrometers as laboratory equipment has been developed. The system ensures the data collection within the process of model objects disintegration, as well as their transmission on USB channels into personal computer.

Fig. 11. Position sensor for mining applications

7. 3D OPTICAL TECHNOLOGIES FOR ATOMIC INDUSTRY

Safety of nuclear reactors and ensuring their high exploitation take 100 % noncontact inspection of fuel assemblies, fuel elements, grid spacers and also fuel element surface inspection with micron resolution. For solving these tasks we have developed and produced for Russian atomic plants some measuring technologies and systems using shadow, low-coherent, structured illumination methods. Among these systems is laser measuring machine (LMM) for inspection of all geometrical parameters of the grid spacer– honeycomb object with more than 300 cells with diameter about 9 mm and in height 20 mm (Fig. 12).

Fig. 12. Laser measuring machine for noncontact fast 3D grid spacer inspection

It is important that LMM can reconstruct any cell profile (Fig. 13). This machine productivity is 10 min, which is more than 300 times faster than existing

universal contact coordinate measuring machines. We have developed and created industrial version of the low-coherent profilometer PROFILE for 3D surface inspection with resolution of 0.1 μm and depth range up to 10 mm. For fuel elements inspection of nuclear

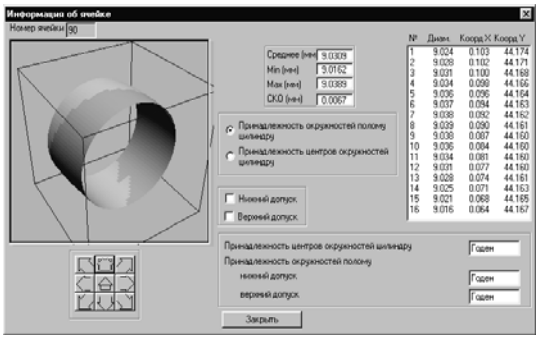

Fig. 13 3D cell profile reconstruction by LMM (fit cell)

reactors VVER-1000 and VVER-440 the opto-electronic automatic measuring device CONTROL using shadow techniques has been developed. The created devices are incorporated directly in the technological lines of fuel element manufacturing.

8. LASER WHEEL PAIRS DIAGNOSTIC INSPECTION FOR RUNNING TRAINS

Ensuring the safety of running trains takes regular inspection of wheels for defects detection. We have developed high-speed laser noncontact method for geometrical parameters inspection of moving 3D objects on the base of triangulation position sensors (Fig. 14) using fast-response PSD linear arrays (10^5 meas/s) (Baybakov et al., 2004).

Figure 15 shows an example of the wheel reconstructed profile (cross-section). The required geometrical parameters are calculated from the reconstructed profile, in so doing, the algorithm of calculating the parameters follows the method of their measurement by means of a standard contact meter.

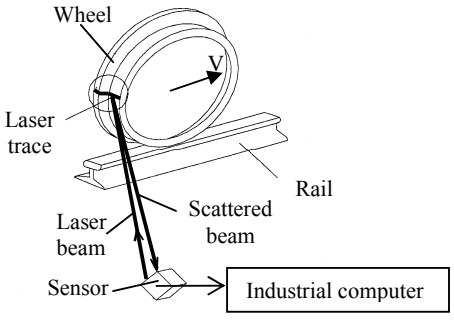

Fig. 14. The principle of self-scanning of running freight car wheels using triangulation measuring sensors.

TDI SIE has developed and produced the automatic laser diagnostic system COMPLEX (Fig. 16) for noncontact inspection of geometric parameters of wheel pairs including: width and thickness of wheel rim; distance between inner sides of wheels; thickness of

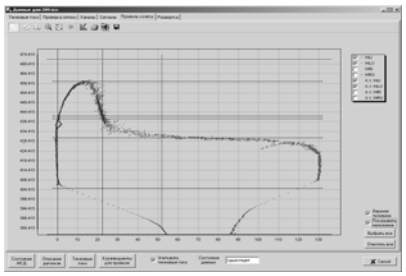

Fig15. A wheel reconstruction profile (cross-section)

wheel flange; uniform rolling; wheel diameter; and axle sliding-off. Measurements are fulfilled at freight cars speed up to 60 km/hr. The range of working temperatures is from –50° up to +50° C.

At the present time 34 systems COMPLEX are in operation on 10 Russian Railways (from Moscow to Far East). Using these systems allows us to increase the safety of railway industry in Russia.

Fig. 16. Automatic laser system for noncontact wheel pairs freight car inspection for running trains.

9. CONCLUSION

New measurement approaches using 3D diffraction results, Fresnel diffraction and diffraction optical elements are promising for 1D, 2D and 3D inspection. We have developed, implemented and tested in real workshop and outside conditions some novel optical measuring systems and laser technologies, which are operating successfully in many fields including mining, atomic, railway and other industries.

10. REFERENCES

Baybakov, A. N.; Gurenko, V. M.; Paterikin, V. I.; Yunoshev, S. P.; Plotnikov, S. V.; Sotnikov, V. V. & Chugui, Yu. V. (2004). Automatic control of geometrical parameters of wheel pairs during train operation. *Optoelectronics, Instrumentation and Data Processing*, Vol. 40, No. 5, pp. 75-82.

Brown, G.M.; Harding, K.G. & Stahl H.P. (1992) Industrial Application of Optical Inspection, Metrology, and Sensing, *Proc. SPIE***,** Vol. 1821.

Chugui, Yu. V.; Yakovenko, N. A. & Yaluplin M. D. (2006). Metrology for Fresnel measuring method, *Measurement Science and Technology*, Vol. 17, pp. 592-595.